ChemComm

Accepted Manuscript

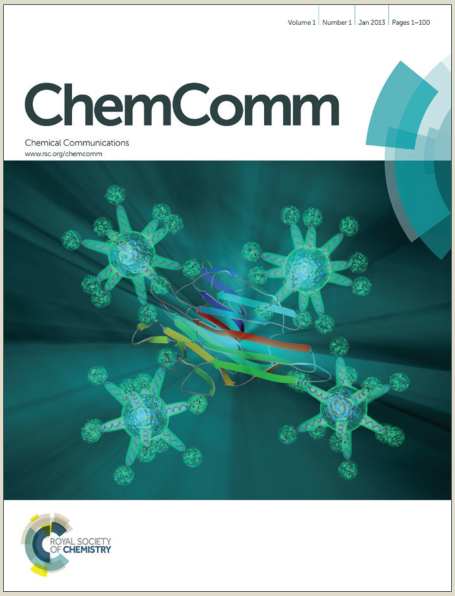

ROYAL SOCIETY OF CHEMISTRY

www.rsc.org/chemcomm

Chemical Communications RSCPublishing

COMMUNICATION

Cite this: DOI: 10.1039/x0xx00000x

Two Modes of Photoinduced Twisted Intramolecular Charge Transfer in *meso*-Arylaminated Subporphyrins

Won-Young Cha,[a] Jong Min Lim,[a] Kyu Hyung Park,[a] Masaaki Kitano,[b] Atsuhiro Osuka,*[b] and Dongho Kim*[a]

Received 00th January 2012,
Accepted 00th January 2012

DOI: 10.1039/x0xx00000x

www.rsc.org/

Photoinduced twisted intramolecular charge transfer (TICT) of *meso*-(4-dimethylamino)phenylamino subporphyrin 2 and *meso*-(4-nitro)phenylamino subporphyrin 3 has been revealed by steady-state and time-resolved absorption/fluorescence experiments and quantum calculations. Subporphyrins 2 and 3 undergo molecular twisting at C_{meso}—N bond and N—C_{ipso} bond, respectively, to trigger intramolecular charge separation, which is restricted at low temperature or in viscous paraffin oil with concurrent fluorescence recovery of local excited states.

In recent years, subporphyrins, ring-contracted porphyrins that can be delineated as [14]triphyrins(1.1.1), have emerged as novel functional pigments.[1-3] As an attractive attribute that is not shared with porphyrins, *meso*-substituted subporphyrins exhibit remarkably variable absorption and fluorescence spectra depending upon *meso*-substituents. In other words, the electronic interactions between the subporphyrin core and the *meso*-substituents are fairly strong to perturb the optical properties of subporphyrin but can be drastically attenuated, for instance, by twisting of the *meso*-substituent from its optimized orientation. During the last several years, new *meso*-substituted subporphyrins have been continuously synthesised but studies on the photophysical properties of subporphyrins have still remained at quite an unexplored level, as compared with porphyrins.

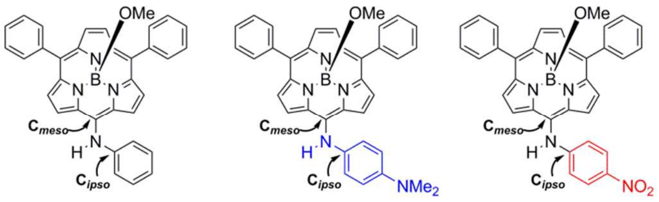

Scheme 1. Molecular structures of *meso*-arylaminated subporphyrins

In our recent work, we reported that intramolecular charge transfer interaction of *meso*-substituted subporphyrins can influence the two photon absorption (TPA) processes due to their directional polarization along the attached electron donating and withdrawing substituents.[4]

In this paper, we have investigated the photodynamics of *meso*-arylaminated subporphyrins **1**, **2**, and **3** (Scheme 1),[5] and found two different TICT processes for **2** and **3**, respectively. Intriguingly, these subporphyrins showed structural distortions due to strong conjugative interactions; subporphyrins **1** and **2** display distinctly shorter C_{meso}—N bonds than N—C_{ipso} due to the strong electron donating interaction of the *meso* arylamino group but subporphyrin **3** shows shorter N—C_{ipso} bond than C_{meso}—N bond due to the electron withdrawing interaction of the 4-nitrophenyl group. In TICT, intramolecular charge separation occurs with twisting of a donor-acceptor arrangement to minimize the electronic interactions.[6] While many luminescent TICT states are known, some TICT states are non-luminescent and responsible for rapid nonradiative decay of dyes. TICT has been demonstrated in many chemical systems but quite rare in porphyrinoid systems.[7]

---

[a] *Department of Chemistry and Spectroscopy Laboratory for Functional π-Electronic System, Yonsei University 262 Seongsanno, Seodaemun-gu, Seoul 120-749 (Korea)*
E-mail: dongho@yonsei.ac.kr
[b] *Department of Chemistry, Graduated School of Science, Kyoto University, Sakyo-ku, Kyoto 606-8502 (Japan)*
E-mail: osuka@kuchem.kyoto-u.ac.jp

Meso-arylaminated subporphyrins **1**, **2** and **3** showed fluorescence properties that are drastically different from that of *meso*-triphenyl substituted subporphyrin.[5] Subporphyrin **1** displayed a broad and red-shifted Soret-like band, and an intensified and red-shifted Q-like band. Characteristically, the fluorescence of **1** was intensified and red-shifted (Figure 1). The fluorescence quantum yields of **1** were recorded to be rather high, 0.47 in toluene and 0.42 in acetonitrile. While the absorption spectra of subporphyrins **2** and **3** are similar to that of **1**, these molecules are practically non-fluorescent; the fluorescence quantum yields of both **2** and **3** are $< 10^{-4}$.

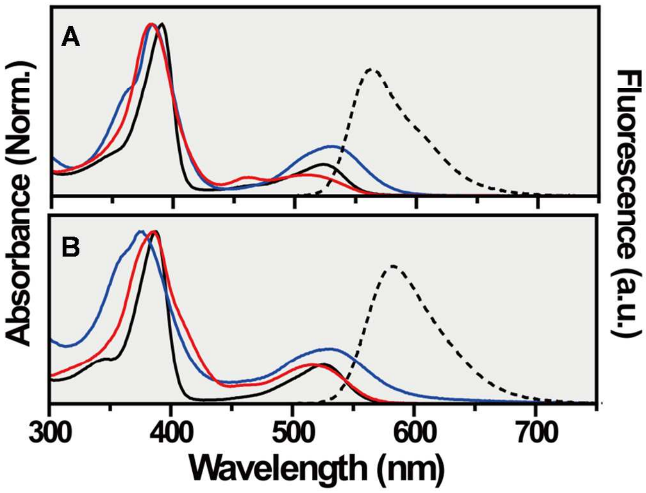

Figure 1. Steady state absorption (solid lines) and fluorescence (dotted lines) spectra of **1** (black), **2** (blue) and **3** (red) in toluene (A) and acetonitrile (B). Both **2** and **3** revealed negligible fluorescence in both solvents. Excitation wavelength is 480 nm.

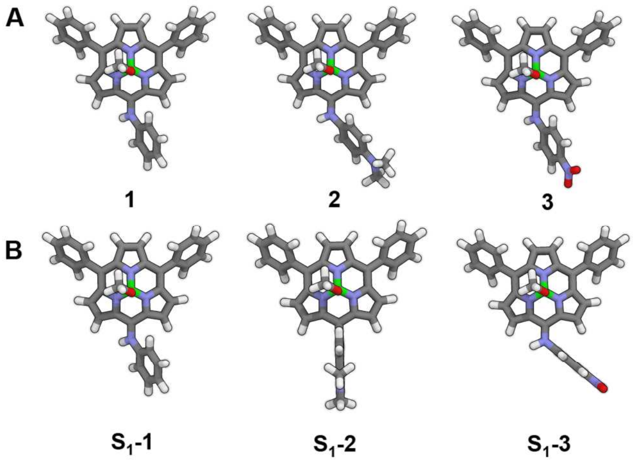

Figure 2. Energy-minimized geometries of ground states (A) of **1**, **2** and **3** and excited states (B) of **S$_1$-1**, **S$_1$-2** and **S$_1$-3**. Optimizations of ground and excited state geometries were calculated at B3LYP/6-31G(d) and RB3LYP/6-31G(d) level, respectively.

To gain insight into the different fluorescence properties of **1-3**, we have calculated the energy-minimized structures both in the ground and exited states by starting from the respective X-ray crystal structure. In the crystals, the dihedral angles of the arylamino groups and the subporphyrin plane are 59, 57 and 46° for **1-3**, respectively.[5] In the energy-minimized structures in the ground state, the dihedral angles are 62, 57 and 55° (Figure 2). On the basis of these structures, the energy-minimized structures of the S$_1$ states of **1-3** (**S$_1$-1**, **S$_1$-2** and **S$_1$-3**) have been calculated. While the optimized structure of **S$_1$-1** was calculated to be almost the same as the ground state structure of **1**, those of **S$_1$-2** and **S$_1$-3** were calculated to have the dihedral angles of ca. 90° as shown in Figure. 2. Importantly, the twisting bond is different; C$_{meso}$—N bond in **S$_1$-2** versus N—C$_{ipso}$ bond in **S$_1$-3**. Although we used several input structures that are slightly different from the optimized ground state structures of **1**, **2** and **3,** our calculation results have been converged to the same structures in all cases. It is worthy to note that the twisting bonds are considered to possess certain double bond character in the ground state on the basis of the distinctly short bond lengths.[5] Such strong bonds in the ground states are weakened and twisted in the excited states. These significant structural changes calculated for **S$_1$-2** and **S$_1$-3** strongly suggest TICT phenomena in their excited state dynamics.[6-9]

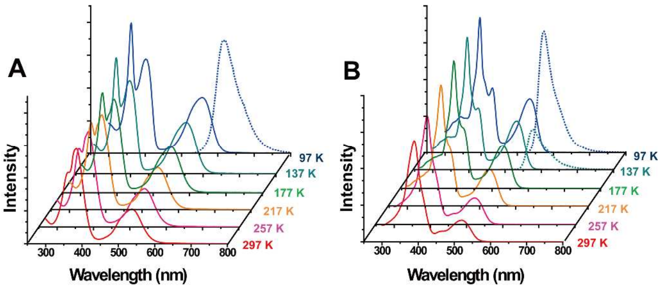

Figure 3. Temperature-dependent steady state absorption (solid line) and fluorescence (dotted line) spectra of **2** (A) and **3** (B) in 2-MeTHF. Excitation wavelength is 480 nm.

To confirm TICT, we have carried out temperature dependent and viscosity controlled experiments to restrict structural changes in the excited state. The absorption and fluorescence spectra of **1**, **2** and **3** were measured between 97 and 297 K (Figure 3 and Figure S1). As the temperature decreased from 297 to 97 K, **1** showed continuous and gradual changes in the absorption and fluorescence spectra but these changes were only modest. Upon similar cooling, the absorption spectra of **2** and **3** exhibited modest changes that are similar to those of **1**, but the fluorescence spectral changes of **2** and **3** are drastically different from those of **1**, revealing fluorescence recovery at low temperature. These results suggest that the restricted rotational freedom in the locally excited state (LES) prevents the intramolecular charge separation (CS). Furthermore, highly viscous paraffin oil was used to ensure the involvement of the rotational motion in the intramolecular CS. Actually, the fluorescence quantum yields of **2** and **3** were recovered up to 0.15 and 0.32, respectively, in paraffin oil (Figure S2).

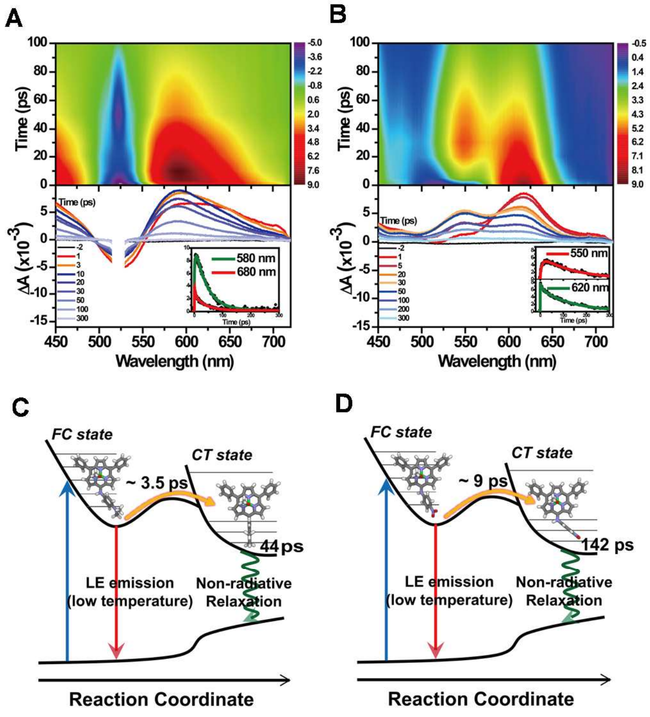

Figure 4. Transient absorption spectra in toluene and schematic representations of the TICT processes of **2** (A, C) and **3** (B, D). Insets are rise and decay profiles. Excitation wavelength is 520 nm.

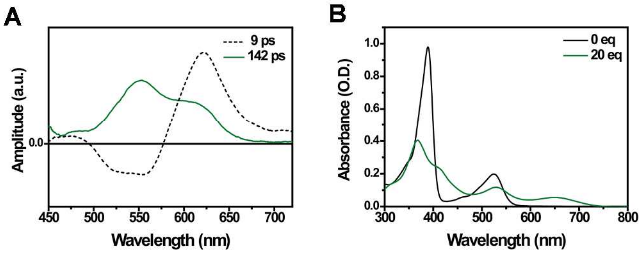

Figure 5. (A) Decay-associated spectra obtained from global multiexponential analysis of the TA spectra of **3** in toluene. (B) Absorption spectra of neutral (black line) and oxidized (green line) **1**.

To gain more detailed information on the TICT processes, we have examined the excited state dynamics of **1**, **2** and **3** in toluene and paraffin oil by femtosecond transient absorption (TA) measurements. In toluene, **1** showed slow TA decay in line with its long fluorescence lifetime and high fluorescence quantum yield (Figures S3-4), but **2** and **3** exhibited significantly faster decay dynamics (Figure 4), which clearly showed that LES of **2** and **3** returned to the ground state rapidly through distinct intermediate states. The positive bands around 700 nm (reddish spectra) in the early TA spectra of **2** and **3**, which have been assigned as LES absorption, disappeared quickly. Through the global analysis, two decay-associated spectra have been extracted for **2** and **3** as shown in Figure S5 and Figure 5A, respectively. The decay-associated spectra of **2** and **3** at early time delays reveal broad and red-shifted ESA signals, whereas the TA spectra at longer time delays show blue-shifted ESA signals. In the case of **2**, the rise and decay profiles of **2** (inset) probed at 580 and 680 nm were well fitted by two exponential functions with the time constants of 3.5 and 44 ps. The TA decay in the region from 650 to 720 nm and newly created positive signals around 590 nm after photoexcitation indicates that as the excited state absorption of LES becomes diminished, that of charge separated state (CSS) grows. The time constant of 3.5 ps indicates that the formation time of charge separated state involves the structural twisting motion at the nitrogen. In the case of **3**, the two decay-associated spectra were also extracted with time components of 9 and 142 ps, and the rise and decay profiles probed at 550 and 620 nm were well fitted by the same time components. The short time constant of 9 ps which corresponds to the decay and rise times of excited state absorption signals (reddish spectra) around 620 and 550 nm, respectively, also indicates that the population of LES is transferred to the CSS. Interestingly, different twisting bonds between $\mathbf{S_1}$**-2** and $\mathbf{S_1}$**-3** (Figure 2) may be related to the different formation time of CSS. Twisting motion at the directly *meso*-bonded nitrogen atom that has structural flexibilities is relatively easier than that at the sp^2 hybridized carbon atom of the benzene ring.

Subporphyrins **1**-**3** showed large Stokes shifts, also indicating large structural changes in their excited states. This situation makes the estimation of the excitation energies of $\mathbf{S_1}$**-1**, $\mathbf{S_1}$**-2**, and $\mathbf{S_1}$**-3** difficult, which were estimated on the basis of the midpoints between the absorption and fluorescence peaks to be 2.23, 2.09, and 2.24 eV, respectively. The electrochemical potentials of **1**, **2**, and **3** were measured by cyclic voltammetry experiments in CH_2Cl_2 (Figure S6). The first oxidation and reduction potentials were observed at 0.22, –0.18, and 0.42 V and at –2.05, –2.14, and –1.87 V, respectively. The first oxidation potentials correspond to the oxidation at the subporphyrin, and hence follow the substituent effect nicely. In other words, the substituent effects of 4-dimethylamino and 4-nitro groups at the arylamino group influence the first oxidation potentials. Similarly, the reduction potentials follow the substituent effects exactly in an opposite manner. On the basis of the electrochemical data, the energy levels of CSS have been estimated to be 2.27, 1.96, and 2.29 eV for **1**-**3**, respectively. It is important to point out that these electrochemical potentials reflect the conjugative interactions of the *meso*-arylamino substituents and the subporphyrin core. In the case of **3**, the twisting at N—C_{ipso} bond is expected to cause disruption of such conjugative interactions. Namely, the donor part, the subporphyrin core of **3** becomes more electron rich because of the suppression of the electron withdrawing interactions of the 4-nitrophenyl group, and the acceptor part, the 4-nitrophenyl group of **3** becomes more electron deficient because of the suppression of electron donating *meso*-amino group. In other words, the twisting triggers the intramolecular CS by disrupting the conjugative interactions. Similar scenario can be considered also for **2**, for which the intramolecular CS is already exothermic without twisting. Twisting at C_{meso}—N bond causes a situation that the subporphyrin core becomes more electron deficient because of the suppression of the electron donating interactions of (4-diemthylamino)phenylamino group and the donor part becomes more electron rich because of the suppression of the electron withdrawing interaction of the deficient subporphyrin core.

We tried to find an evidence for the formation of intermediate charge separated species, i.e. subporphyrin cation radical, by monitoring the spectral features of newly generated excited state absorption bands. In this regard, we obtained the steady state absorption spectrum of chemically oxidized subporphyrin **1** by titration of $NOSbF_6$ in dichloromethane/acetonitrile (1:1), in which oxidized species, cation radical of *meso*-arylaminated subporphyrin, showed the newly created absorption band ranging from 560 to 700 nm (Figure 5B and Figure S7). It is noteworthy that the positive band ranging from 560 to 700 nm of **3** in the TA spectra at longer delay times becomes similar to that of the cation radical of **1**, which supports the formation of charge separated species in the excited state. In addition, we obtained the TA spectra of **2** and **3** in highly viscous paraffin oil (Figure S8). Similar to the case of **1** in toluene, **2** and **3** showed the slow TA decay without complex excited state dynamics being consistent with the high fluorescence quantum yields of 0.15 and 0.33, respectively. These results indicate that the formations of charge separated states of **2** and **3** are accompanied by the significant structural changes in the excited state.

In conclusion, we have investigated the excited state dynamics of *meso*-arylaminated subporphyrins 1, 2 and 3 by the steady-state and time-resolved absorption and fluorescence spectroscopic measurements along with computational calculations. Photoexcitation of 1 leads to the population of LE that has a slow TA decay and high fluorescence quantum yield. In contrast, upon photoexcitation, 2 is initially excited to its LE that twists the C_{meso}—N bond to trigger the intramolecular CS to give subporphyrin anion radical and 1,4-diaminobenzene cation radical, while 3 is excited to its LE that undergoes twisting of the N—C_{ipso} bond to trigger the opposite CS to give subporphyrin cation radical and nitrobenzene anion radical. These TICT processes are considerably suppressed at low temperature or in viscous paraffin oil environments. Through this study, subporphyrins have been shown to be a platform of TICT. Along this line, other *meso*- and *beta*-substituted subporphyrins are actively pursued in our laboratories and will be reported elsewhere.

The work at Yonsei was supported by Global Research Laboratory program (2013-8-1472), Mid-carrier Researcher Program (2010-0029668) of National Research Foundation grant funded by MEST of Kore**a.** The work at Kyoto was supported by Grants-in-Aid (No. 25220802 (S)) for Scientific Research from MEXT. M. K. thanks JSPS fellowship for Young Scientists.

Notes and references

1 (a) T. Torres, *Angew. Chem. Int. Ed.,* 2006, **45**, 2834-2837; (b) Y. Inokuma, A. Osuka, *Dalton Trans*., 2008, 2517; (c) A. Osuka, E. Tsurumaki, T. Tanaka, *Bull. Chem. Soc. Jpn.,* 2011, **84**, 679.

2 (a) Y. Inokuma, J. H. Kwon, T. K. Ahn, M.-C. Yoo, D. Kim, A. Osuka, *Angew. Chem. Int. Ed.*, 2006, **45**, 961; (b) N. Kobayashi, Y. Takeuchi, A. Matsuda, *Angew. Chem. Int. Ed.*, 2007, **119**, 758.

3 Y. Inokuma, Z. Yoon, D. Kim, A. Osuka, *J. Am. Chem. Soc.*, 2007, **129**, 4747.

4 (a) Y. Inokuma, S. Easwaramoorthi, S. Jang, K. Kim, D. Kim, A. Osuka, *Angew. Chem. Int. Ed.*, 2008, **120**, 4840; (b) S. Easwaramoorthi, J.-Y. Shin, S. Cho, P. Kim, Y. Inokima, E. Tsurumaki, A.Osuka, D. Kim, *Chem. Eur. J.*, 2009, **15**, 12005.

5 M. Kitano, S. Hayashi, T. Tanaka, N. Aratani, A. Osuka, *Chem. Eur. J.*, 2012, **18**, 8929.

6 W. Rettig, *Angew. Chem. Int. Ed. Engl.*, 1986, **25**, 971.

7 (a) Z. R. Grabowski, K. Rotkiewicz, *Chem. Rev*., 2003, **103**, 3899; (b) T. Fujiwara, C. Reichardt, R. A. Vogt, C. E. Crespo-Hernández, M.Z. Zgierski, E. C. Lim, *Chemical Physics Letters*, 2013, **586**, 70; (c) A. Pedone, *J. Chem. Theory Comput*. 2013, **9**, 4087; (d) D. Maftei, G. Zbancioc, I. Humelnicu, I. Mangalagiu, *J. Phys. Chem. A*, 2013, **117**, 3165; (e) C.-K. Lin, Y.-F. Wang, Y.-C. Cheng, J.-S. Yang, *J. Phys. Chem. A*, 2013, **117**, 3158; (f) M. Park, C. H. Kim, T. Joo, *J. Phys. Chem. A*, 2013, **117**, 370; (g) S. Rafiq, R. Yadav, P. Sen, *J. Phys. Chem. A*, 2011, **115**, 8335; (h) R. Karpicz, S. Puzinas, S. Krotkus, K. Kazlauskas, S. Jursenas, J. V. Grazulevicius, S. Grigalevicius, V. Gulbinas, *J. Chem. Phys.*, 2011, **134**, 204508.

8 I. Pugliesi, U. Megerle, S-L. Suraru, F. Würthner, E. Riedle, S. Lochbrunner, *Chem. Phys. Lett.*, 2011, **504**, 24.

9 I. Pugliesi, P. Krok, S. Lochbrunner, A. Blaszczyk, C. Hanisch, M. Mayor, E. Riedle, *J. Phys. Chem. A*, 2010, **114**, 12555.